Seasonally decoupled dynamics of dissolved organic carbon and fluorescent dissolved organic matter in continental shelf waters

Heejun Han[1], Hyung-Mi Cho[2*], Jeomshik Hwang[3], Hanbyul Lee[3], Guebuem Kim[3]

[1]Marine Environmental Research Department, Korea Institute of Ocean Science and Technology (KIOST), Busan 49111, South Korea

[2]Department of Ocean Sciences, Inha University, Incheon 22212, South Korea

[3]School of Earth and Environmental Sciences/Research Institute of Oceanography, Seoul National University, Seoul 08826, Republic of Korea

Figure S1. Surface contour plots of salinity, DOC concentration, $SUVA_{350}$, FDOM components (C peak, T peak, and M peak), S_R, $S_{275–295}$, and $S_{350–400}$ values in winter (February 2017).

Figure S2. Surface contour plots of salinity, DOC concentration, $SUVA_{350}$, FDOM components (C peak, T peak, and M peak), S_R, $S_{275–295}$, and $S_{350–400}$ values in spring (April 2018).

Figure S3. Surface contour plots of salinity, DOC concentration, $SUVA_{350}$, FDOM components (C peak, T peak, and M peak), S_R, $S_{275–295}$, and $S_{350–400}$ values in summer (August 2020).

Figure S4. Surface contour plots of salinity, DOC concentration, $SUVA_{350}$, FDOM components (C peak, T peak, and M peak), S_R, $S_{275–295}$, and $S_{350–400}$ values in fall (November 2021).

Figure S5. Surface contour plots of salinity, DOC concentration, $SUVA_{350}$, FDOM components (C peak, T peak, and M peak), S_R, $S_{275–295}$, and $S_{350–400}$ values in summer (July 2022).

Figure S6. Vertical profiles of (a) salinity, (b) DOC concentration, (c) $FDOM_H$ components, (d) S_R, (e) $S_{275–295}$, and (f) $S_{350–400}$ values in the northwestern Pacific marginal seas during the sampling periods.

Table S1. The minimum, maximum, and average salinity, temperature, DOC concentration, FDOM components, S_R, $S_{275–295}$, and $S_{350–400}$ values during spring, summer, fall, and winter.

Radium age calculation method

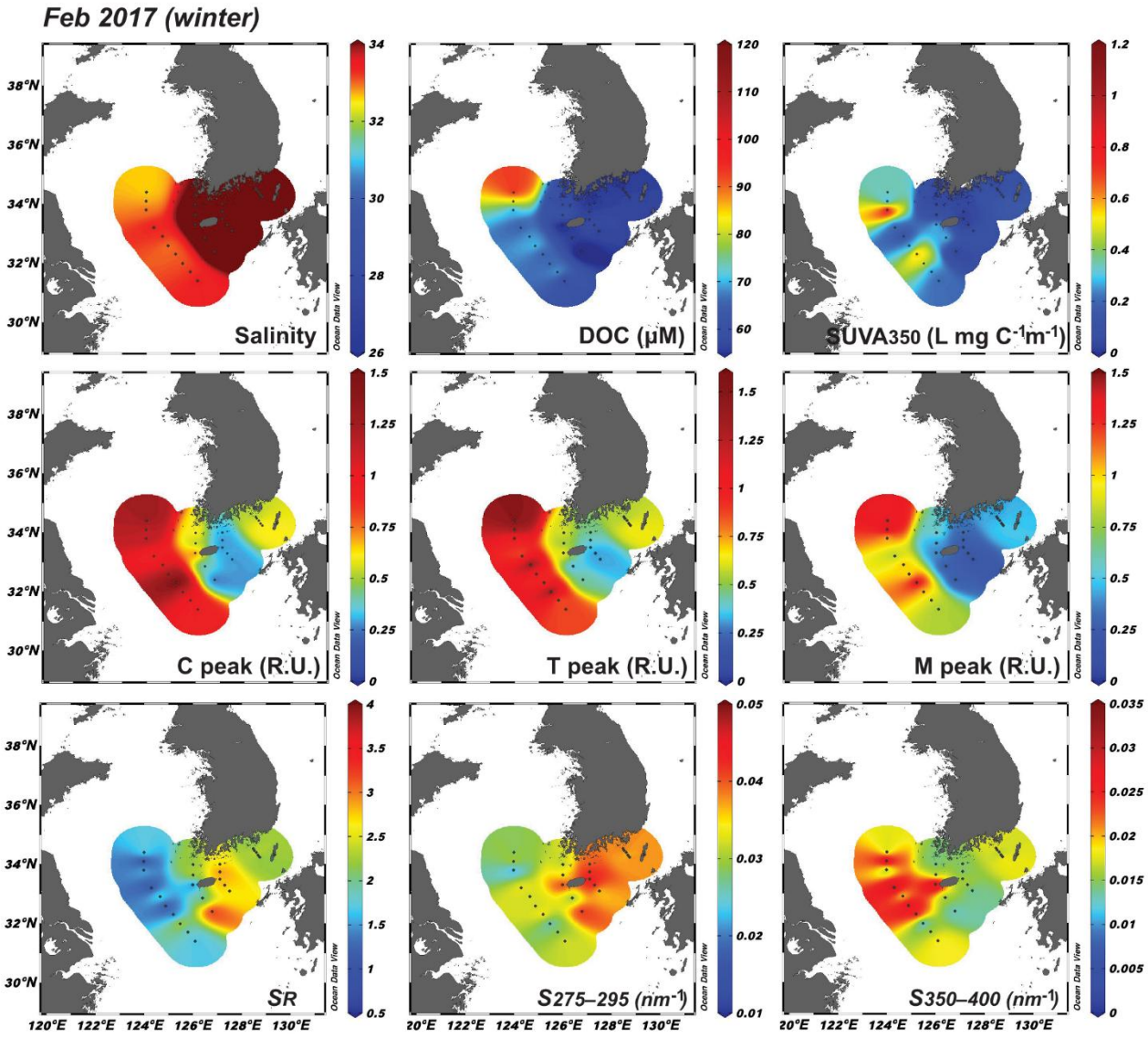


Figure S1. Surface contour plots of salinity, DOC concentration, $SUVA_{350}$, FDOM components (C peak, T peak, and M peak), S_R, $S_{275–295}$, and $S_{350–400}$ values in winter (February 2017).

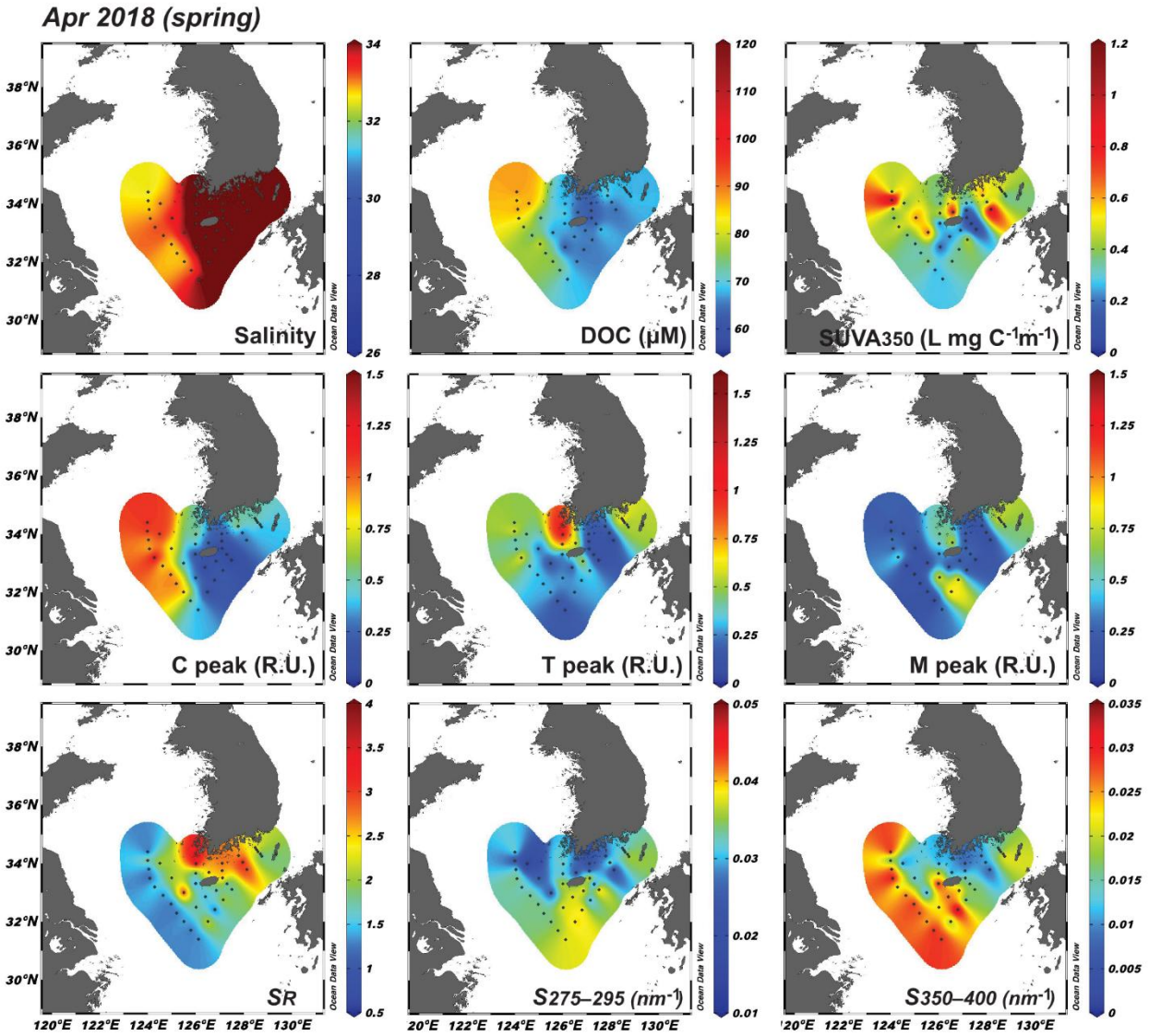


Figure S2. Surface contour plots of salinity, DOC concentration, $SUVA_{350}$, FDOM components (C peak, T peak, and M peak), S_R, $S_{275–295}$, and $S_{350–400}$ values in spring (April 2018).

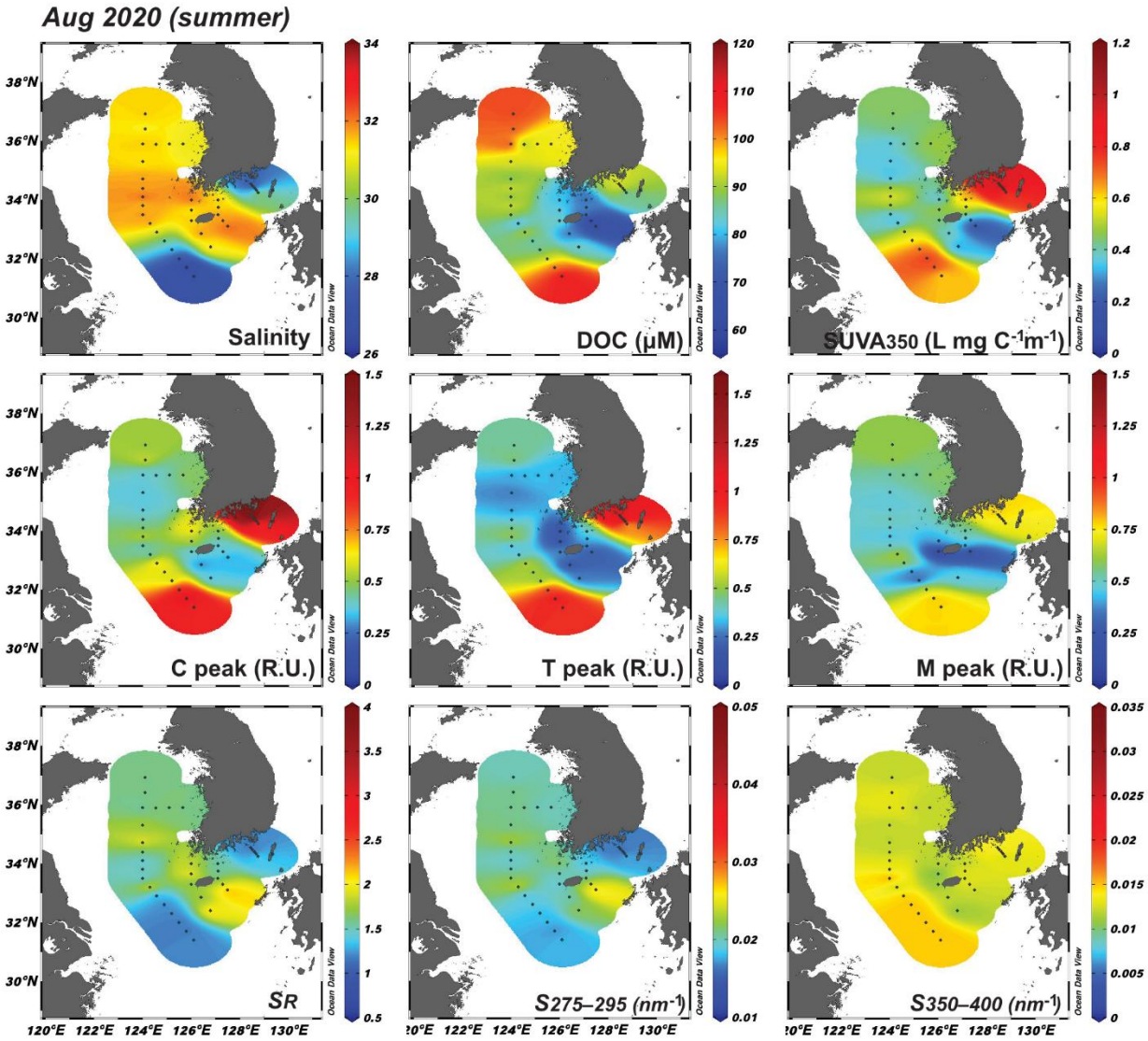


Figure S3. Surface contour plots of salinity, DOC concentration, $SUVA_{350}$, FDOM components (C peak, T peak, and M peak), S_R, $S_{275–295}$, and $S_{350–400}$ values in summer (August 2020).

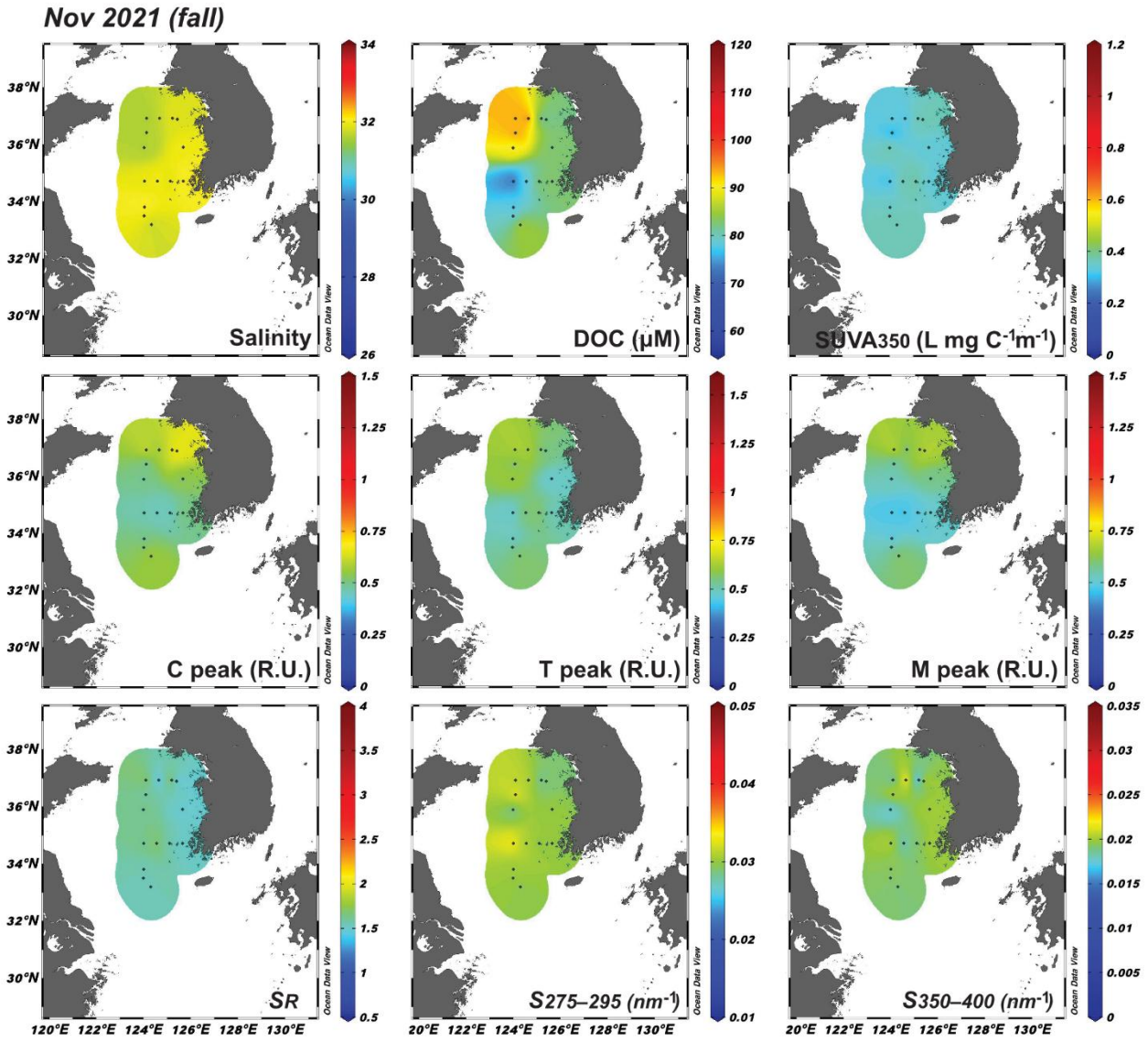


Figure S4. Surface contour plots of salinity, DOC concentration, $SUVA_{350}$, FDOM components (C peak, T peak, and M peak), S_R, $S_{275–295}$, and $S_{350–400}$ values in fall (November 2021).

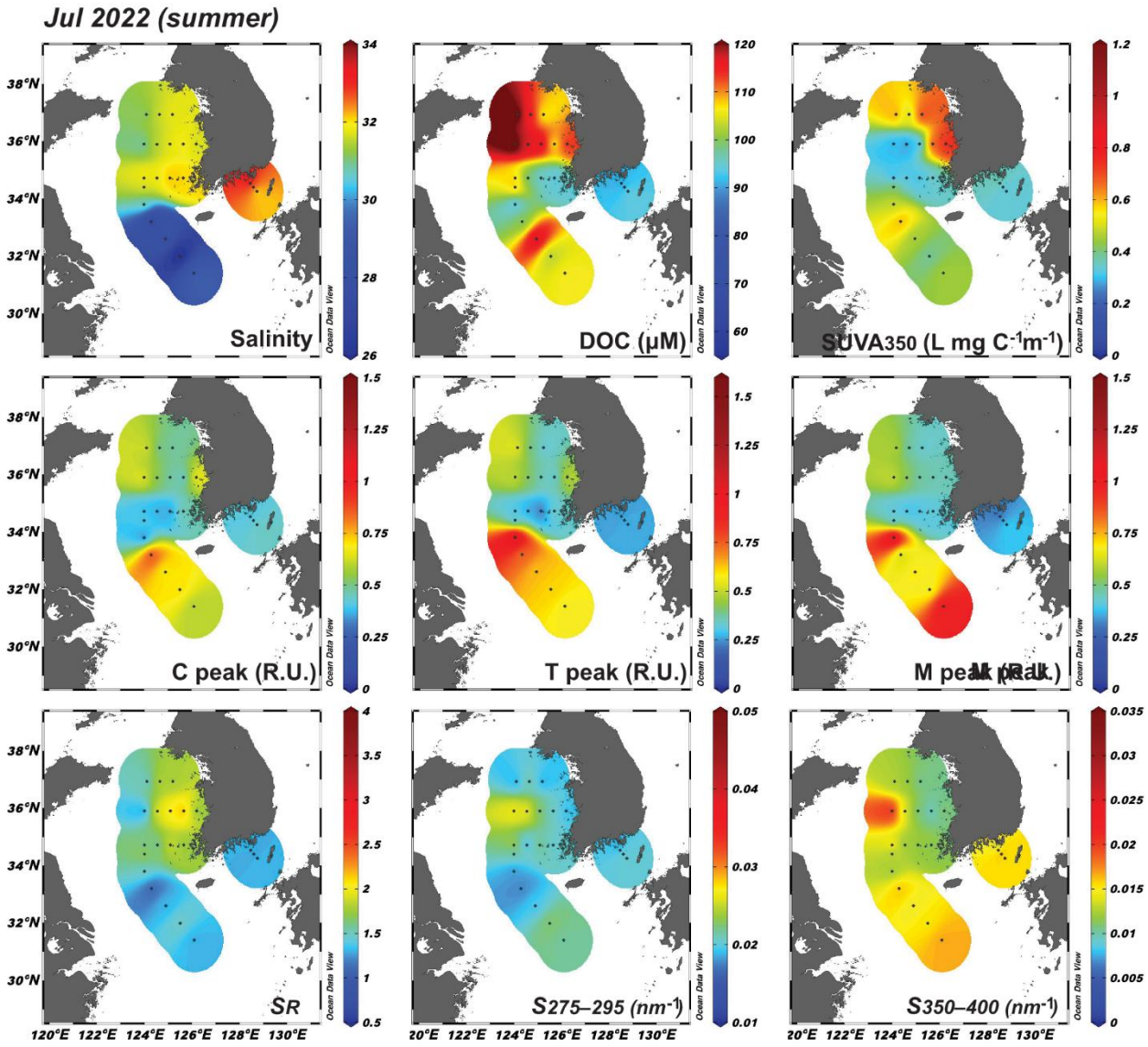


Figure S5. Surface contour plots of salinity, DOC concentration, $SUVA_{350}$, FDOM components (C peak, T peak, and M peak), S_R, $S_{275–295}$, and $S_{350–400}$ values in summer (July 2022).

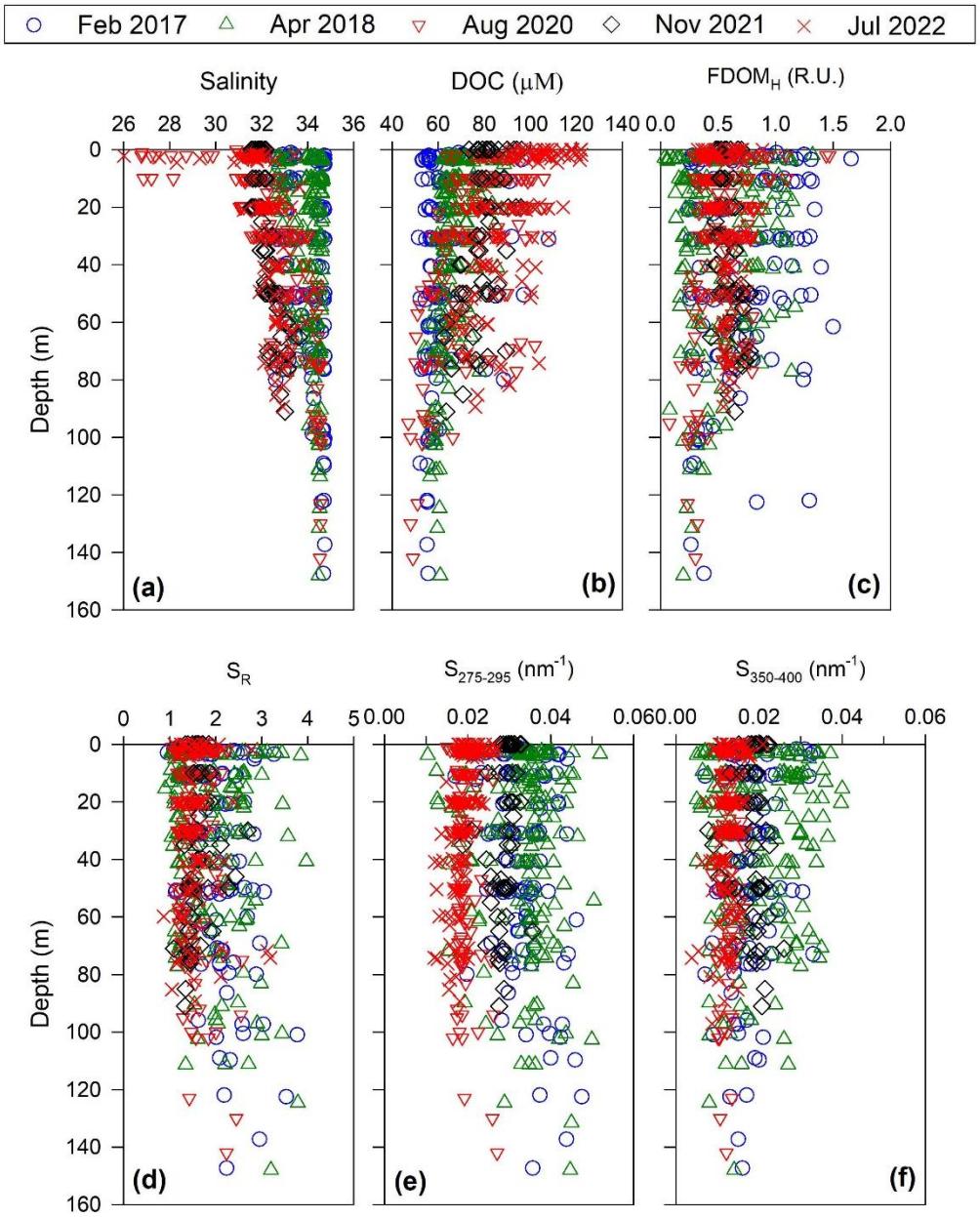


Figure S6. Vertical profiles of (a) salinity, (b) DOC concentration, (c) $FDOM_H$ components, (d) S_R, (e) $S_{275–295}$, and (f) $S_{350–400}$ values in the northwestern Pacific marginal seas during the sampling periods.

Table S1. The minimum, maximum, and average salinity, temperature, DOC concentration, FDOM components, S_R, $S_{275–295}$, and $S_{350–400}$ values during spring, summer, fall, and winter.

Season		Salinity	Temp. (°C)	DOC (μM)	$FDOM_H$ (R.U.)	$FDOM_P$ (R.U.)	$FDOM_{H2}$ (R.U.)	S_R	$S_{275–295}$	$S_{350–400}$
Winter	Min–Max	32.60–34.73	9.26–17.29	51–108	0.24–1.66	0.23–1.55	0.17–1.46	0.954–3.772	0.017–0.048	0.007–0.033
(Feb 2017)	Avg. ±SD	33.98±0.72	13.49±2.41	62±10	0.73±0.37	0.54±0.27	0.51±0.30	2.019±0.572	0.034±0.006	0.018±0.006
Spring	Min–Max	32.46–34.65	7.75–18.53	54–89	0.04–1.32	0.05–2.05	0.02–1.85	0.435–6.114	0.009–0.061	0.003–0.098
(Apr 2018)	Avg. ±SD	34.02±0.62	13.64±2.46	67±7	0.54±0.31	0.38±0.33	0.41±0.37	1.905±1.056	0.034±0.009	0.025±0.019
Summer	Min–Max	26.77–34.57	8.85–29.46	47–109	0.18–1.47	0.06–1.68	0.07–1.26	1.054–2.570	0.015–0.027	0.009–0.017
(Aug 2020)	Avg. ±SD	32.26±1.68	19.87±5.92	77±16	0.53±0.21	0.48±0.23	0.49±0.20	1.521±0.286	0.019±0.002	0.013±0.002
Fall	Min–Max	31.55–33.60	8.74–18.12	63–96	0.42–0.74	0.33–0.70	0.38–0.76	1.091–2.696	0.019–0.036	0.008–0.026
(Nov 2021)	Avg. ±SD	32.23±0.47	14.01±2.17	80±8	0.57±0.09	0.49±0.09	0.59±0.10	1.615±0.279	0.029±0.003	0.018±0.003
Summer	Min–Max	26.01–34.25	8.14–28.83	58–122	0.29–0.89	0.21–1.12	0.05–1.16	0.868–3.186	0.012–0.027	0.004–0.021
(Jul 2022)	Avg. ±SD	32.23±1.22	17.16±6.39	93±15	0.55±0.13	0.47±0.14	0.42±0.17	1.569±0.378	0.019±0.003	0.012±0.003

Radium age calculation method

The apparent age of water in the YS was calculated using the mass balance of ^{228}Ra and ^{226}Ra, the relationship between the excess Ra isotopes and the Ra fluxes, based on Kim et al.[1]'s approach in the same study area. In this study, we revisit the evaluation of the excess input flux of Ra in a mixture of Kuroshio water and Yangtze River water by incorporating additional data obtained from this study, despite the previous assessment conducted by Kim et al.[1].

To establish a mass balance for ^{226}Ra in surface waters, we considered all sources including the Yangtze River water, desorption from sediments and dust, the Kuroshio water, submarine groundwater discharge (SGD), and diffusion from bottom sediments. These sources were divided into two categories: (1) a conservative fraction, combining Kuroshio and Yangtze River waters, and (2) an excess fraction from SGD, and desorption of suspended sediments, dust, and bottom sediments. The equations (1) and (2) may express the observed activity (Ra_o) for ^{226}Ra and ^{228}Ra:

$$^{226}Ra_o = f\,^{226}Ra_K + (1-f)\,^{226}Ra_{YR} + {}^{226}Ra_{ex} \quad (1)$$

$$^{228}Ra_o = f\,^{228}Ra_K + (1-f)\,^{228}Ra_{YR} + {}^{228}Ra_{ex} \quad (2)$$

where Ra_o, Ra_K, Ra_{YR}, and Raex represent the observed Ra activities in the YS water, Kuroshio water and Yangtze River endmembers, and the excess Ra activity, respectively. The fraction of the Kuroshio endmember, f, is calculated based on the salinity of the measured values relative to the salinity of Kuroshio surface water.

The endmember values of salinity, $^{226}Ra_K$, and $^{228}Ra_K$ were estimated as 34.5, 6.9, and 2.2 dpm 100 L^{-1}, respectively, according to values from previous studies[1,2]. The endmember values of salinity, $^{226}Ra_{YR}$, and $^{228}Ra_{YR}$ were assumed to be 0, 10, and 19 dpm 100 L^{-1}, respectively[1,2]. Then, $^{226}Ra_{ex}$ and $^{228}Ra_{ex}$ values can be calculated using these endmembers and equations (1) and (2).

The relationship between the excess Ra isotopes and the Ra fluxes can be indicated through equations (3) and (4) under steady state:

$$^{226}Ra_{ex} = \left(F_{226} - \lambda_{226}\,^{226}Ra_o\right)\tau_w \quad (3)$$

$$^{228}Ra_{ex} = \left(F_{228} - \lambda_{228}\,^{228}Ra_o\right)\tau_w \quad (4)$$

where F and λ are the total flux of excess Ra (F_{226} for ^{226}Ra; F_{228} for ^{228}Ra) and the decay constants of Ra (λ_{226} for ^{226}Ra; λ_{228} for ^{228}Ra), respectively. τ_w is the water residence time. In the equation (3), the λ_{226} $^{226}Ra_o$ is negligible due to the long half-life of ^{226}Ra ($t_{1/2}$=1600 yr). Then, equations (3) and (4) can be reorganized to:

$$\frac{^{228}Ra_{ex}}{^{226}Ra_{ex}} = \frac{F_{228}}{F_{226}} - \left(\frac{\lambda_{228}}{F_{226}}\right)\,^{228}Ra_o \quad (5)$$

Using the intercept and slope of the relationship between $^{228}Ra_{ex}/^{226}Ra_{ex}$ and ^{228}Ra activity (Fig. S8),

the estimated excess flux of ^{226}Ra is approximately 6.5 dpm 100 L^{-1} yr^{-1}. The water residence times are then calculated to range from 1.3 to 4.6 years, which falls within the range of residence time for YS water, estimated to be 5–6 yr[1,2].

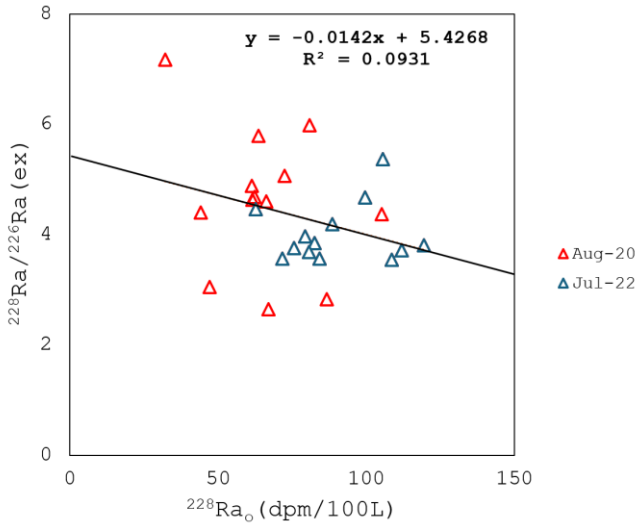


Figure S8. A plot of $^{228}Ra_{ex}/^{226}Ra_{ex}$ versus observed ^{228}Ra activity. The data for the red and blue triangles are from August 2020 and July 2022, respectively. The slope and intercept of this regression curve are used for calculating Ra fluxes in the Yellow Sea based on the equation (5).

References

1. Kim, G., Ryu, J.-W., Yang, H.-S. & Yun, S.-T. Submarine groundwater discharge (SGD) into the Yellow Sea revealed by ^{228}Ra and ^{226}Ra isotopes: Implications for global silicate fluxes. *Earth Planet. Sci. Lett.* **237**, 156–166; 10.1016/j.epsl.2005.06.011 (2005).
2. Nozaki, Y., Tsubota, H., Kasemsupaya, V., Yashima, M. & Ikuta, N. Residence times of surface water and particle-reactive ^{210}Pb and ^{210}Po in the East China and Yellow seas. *Geochim. Cosmochim. Acta* **55**, 1265–1272; 10.1016/0016-7037(91)90305-O (1991).